AN EFFICIENT 95-GHZ, RF-COUPLED ANTENNA*

Yasser A. Hussein and James E. Spencer[§], SLAC, Menlo Park, CA 94025, U.S.A.

Abstract

This paper presents an efficient, RF-coupled, 95-GHz undulatory (snake-like) antenna that can be fabricated using IC technology. While there are many uses for directed power at this frequency our interest is in understanding the propagation of the input power through the circuit and its radiative characteristics for comparison to earlier work in the THz range (see PAC05). 95 GHz was chosen because test equipment was available (WR-10 waveguide and HP network analyzer). Different materials, heights and widths of the circuit were considered on a low-loss, 0.10-mm thick quartz substrate of 0.75 μm of elevated gold corresponding to three skin depths. The design is compared to more conventional RF technology using a low energy, high power electron beam and to higher energy, lower power Smith Purcell gratings and free-electron-lasers (FELs). The FDTD results show narrow-band, 80% radiation efficiency with a dipole-like radiation pattern - enhanced by adding periods. Radiated power was calculated using two different techniques that agreed quite well i.e. by integrating the far-field Poynting vector as well as subtracting the output from input power.

INTRODUCTION

Recently, we explored methods for producing narrow-band THz radiation using either free or conduction-band electrons with micro-undulatory structures [1]-[2]. There is a clear need [3] and since the THz gap extends from about 100 GHz to 3 THz, integrated circuit technology could prove well matched to this range given the right mechanism. One can distinguish several ways of making such radiation using molecular lasers, interfering laser beams, free or solid state electrons. Our emphasis is on producing radiation using IC technology as opposed to conventional FELs that are bulky, expensive, need high power and have low efficiencies [4] even though micro-FELs are possible using IC techniques [5].

95 GHz was chosen to allow us to test mechanisms with an available HP 8510 MM-Wave system that includes an S-parameter network analyzer and sources.

Our choice of materials and format is a legacy that severely limits our options e.g. a Si substrate in the form of a waveguide is more versatile because it could serve as a detector as well if the matrix was a superconductor but is far better than SiO_2 for laser excitation of a drive pulse.

While accurate calculations require coupling Maxwell's equations with an appropriate physics-based transport model, we concentrate our electromagnetic analysis on assumptions of ballistic transport and that radiation loss is much greater than other loss mechanisms, i.e. conductor, thermal or substrate losses.

GENERAL DISCUSSION

Throughout this discussion we understand "feature size" to be comparable to one-half wavelength of the undulatory structure ½λ_u where in Fig. 1 we show a 2λ_u structure.
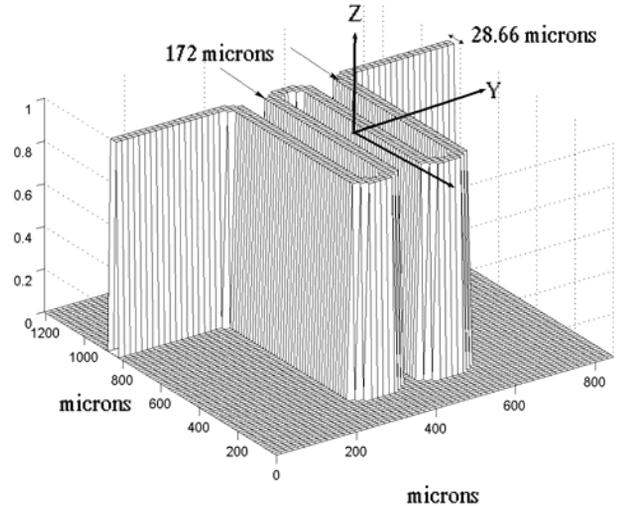
Figure 1: Planar lattice (not to scale) for one cell with the vertical showing gold of 7500 Å height and "0" a low-loss quartz substrate.

Clearly in Fig.1 there are several radiating substructures whose effects produce different wavelengths and spectral characteristics. Differing input and output pad structures will provide short pulse, broadband background differing from the loops in between. These loops are longitudinally separated by λ_l=172 μm and have mean diameters of ½λ_l=86μm. Transversely, they are separated by another design tuning element having a length L=868μm between successive loops at either end. As L→0, quasi-monochromatic light from such structures is expected at a wavelength λ ≈ ½λ_l for sufficiently long pulse excitation. We note that for bound or low energy electrons (E≤100 keV), the normalized energy γ=E/mc², barely reaches 1.2. Further, we estimate that the radiation pulse length for such a loop will have duration:

$$\Delta T(s) = \pi \lambda_l n / 2 \cdot 10^8 [m] \rightarrow 4ps. \qquad (1)$$

Thus, by long pulse we mean τ » 4 ps compared to a single cycle oscillation for λ_l of 0.6 ps. The deflection parameter K=π/2 and the critical frequency ν_c is

$$\nu_c = 3 \ c/(\pi \cdot \lambda_1 \cdot n) \approx c/(\lambda_1 \cdot n) \gg 95 \ GHz. \qquad (2)$$

The lowest frequency structure here that satisfies ωΔT«1 is that for λ_u=½π λ_l + 2L in Fig.1 with a frequency ν near 100GHz as shown below. The angular spread varies with polarization with the σ component better collimated. Most of the radiated energy is confined to ±½π -- improving with the number of cells.

ANTENNA DESIGN

The unit cell in Fig.1 is constructed using four similar sections each of length 1000 microns corresponding to approximately $\lambda/2$ at 95 GHz for an index n=1.58. The non radiative power lost due to surface or bulk waves can be minimized by using a thin substrate, typically $\lambda/10$ or less. However, this depends on how we want to excite the structure since the situation is very different for 95 GHz than for the THz region where we lack good sources. Thus, if we want to excite such structures e.g. using fiber optics and lensing to match into such an aperture, then for a good propagating mode the coupling would be similar to its use as a detector where the coupling is through the evanescent field overlapping the strip-line in the SiO_2.

This layout could be built using a 100 μm thick (~ $\lambda/30$) low-loss quartz substrate. On the other hand, conductor loss is not important at high-frequency since circuit dimensions shrink proportional to the frequency while the skin effect resistance increases proportional to the square root of the frequency. Measurements confirmed this on a test structure done by the authors conducted around 100 GHz using WR-10 setup and HP85106D network analyzer, which showed negligible conductor loss. The characteristic impedance of the input transmission line of the antenna is approximately 121Ω's. Therefore, one needs to use, e.g. a balun, for impedance matching and also to connect the antenna to the excitation source via a CPW or coaxial line.

FDTD CALCULATION&VALIDATIONS

Finite-difference time-domain code was developed to calculate S-parameters as well as radiation patterns and efficiencies. The space steps used were Δx = 14.33 μm, Δy = 14.33 μm and Δz = 33.3 μm. The total mesh dimensions are 85 by 60 by 16 in the x-, y-, and z-directions respectively. The microstrip width is modeled as 2 Δx. The time step is calculated based on the CFL condition to be 0.0193 ps. A Gaussian pulse is used with width of approximately τ=15 ps.
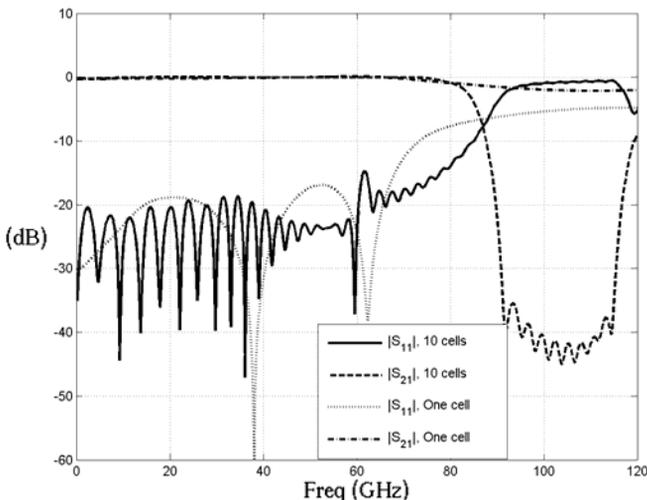
Figure 2: Scattering parameters for one and ten cells from Fig.1

Figure 2 shows the return and insertion loss calculated for the one cell shown in Fig. 1 as well as for a periodic structure composed out of ten such cells. Both the return and insertion losses are more pronounced for the ten-cell case with more resonances corresponding to the number of cells. The return loss (S_{11}) is close to one around 100 GHz. However, the insertion loss (S_{21}) is about -40 dB around 100 GHz, which suggests losses due to radiation that will be verified when the radiated power and patterns are calculated. It is worth mentioning that the values of the scattering parameters for 2-port networks suggest the only possibility is radiation but one needs to estimate the power radiated, i.e. the output power subtracted from the input power for verification. In other words, S-parameters along with circuit impedance can show the full picture. It is also interesting to consider different substrate formats.

Using FDTD, one can calculate both voltages and currents at the input and output ports in time domain, which can be transformed in frequency domain using a Fourier transform that is just the time integral over the pulse for $\omega\Delta T \ll 1$. The input and output power along with the radiation efficiency can then calculated as:

$$P_{in} = V_{in}(f) \cdot I_{in}(f) \qquad (3)$$

$$P_{out} = V_{out}(f) \cdot I_{out}(f) \qquad (4)$$

$$\text{Efficiency} = \frac{P_{in} - P_{out}}{P_{in}} \qquad (5)$$
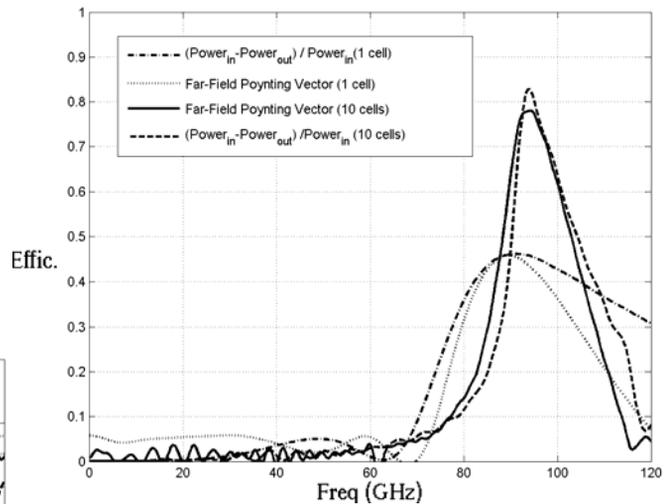
Figure3: Radiation efficiency calculations for one and 10 cells.

The radiation efficiency can alternatively be calculated by integrating the far-field Poynting vector over the entire domain. FDTD code was developed to estimate radiated power based on the algorithm provided by Taflove[6]. Figure 3 shows the radiation efficiency as a function of frequency for the one cell and 10-cell cases using two independent calculations. From Fig. 3, one sees the enhancement of efficiency and bandwidth on adding cells.

The radiation efficiency is around 80% for the 10-cell case, while it is about 40% for the one cell. Further, the bandwidth is much narrower for the 10-cell case. Finally, the radiation efficiency calculations using both techniques agree very well especially for the 10-cell case.

Figure 4 shows the radiation patterns for the one-cell and 10-cell cases. Again, the radiation patterns for both the E- and H-plane are enhanced when adding cells, as predicted. The front-to-back ratio is on average below 10 dB for both planes.
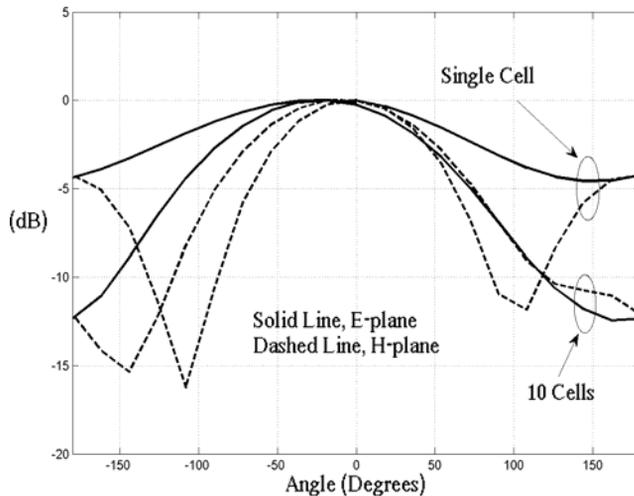
Figure 4: Relative power in dB versus angle (θ) for the one cell and ten-cell cases. Solid line for the E-plane ($\varphi = 90^\circ$), dashed line for the H-plane ($\varphi = 0^\circ$).

CONCLUDING REMARKS

Our primary concern here was to test ideas for solid state THz radiators in a range where existing hardware was available at 100 GHz. While this is on the boundary of the so-called THz gap, it implies a number of serious differences that are related to both Input and Output (I/O) methods. Some of these were discussed. Also, while micro-FELs are possible and interesting based on IC techniques [5], our approach is closer to antenna design but, in fact, could be driven with free electrons as a Smith-Purcell grating. While this would be an interesting test, it would have a poor figure of merit based on power usage and power conversion efficiency.

Previously, we were able to drive amperes of high rep-rate pulses with lengths of a few ns through comparable sized Au trenches in Si wafers (Fig. 5) without failures.

Perhaps of most interest is the underlying physics of such devices i.e. how they are to be excited and what their high frequency response will be. Thus, the materials and structures are very important. Conceptually, it is simpler to assume that the electronic part is a superconducting material to insure ballistic transport and achieve some degree of coherence. However, this ignores many complications, including how one accesses the radiation field. For normal systems, it is not clear whether one prefers the undulatory circuit to be a metal or semiconductor. Based on low frequency mobility,

semiconductors would be the choice but neither is adequate without invoking surface plasma waves or plasmons to reduce the effective impedance. In this way, excitation modes are differentiated e.g. a periodic laser excitation from an oblique angle above the structure that could be matched to the entire length L and width Δx using the Talbot image method [7]. This would be especially interesting for sequential loops such as shown previously in Fig. 2 of Ref. [2].

REFERENCES

[1]   Y. A. Hussein and J. E. Spencer, "Novel Possibilities for Coherent Radiation Sources," *Proc. IEEE MTT-S Int. Sym. Dig.*, 2004, p.365-368.

[2]   Yasser A. Hussein and James E. Spencer, "Calculations for THz Radiation Sources," PAC'05, Knoxville, May 2005, p.1994.

[3]   P. H. Siegel, "Terahertz technology," *IEEE Trans. Micro. Theory Tech.*, 50, No. 3, p. 910-928, 2002.

[4]   Stanford's FIREFLY undulator typically produces $\leq$ 1 W of 15-85 µm radiation with a 30 MeV superconducting linac. FELIX produces 20-250 µm at comparable power in the Netherlands. Modern Editor's Journal 25 (1997) 56.

[5]   J.E. Spencer et al., "Scaling Constraints for Micro-Scale Magnet Structures," PAC'07, Albuquerque, NM, June 2007.

[6]   A. Taflove, *Computational Electrodynamics: The Finite Difference Time Domain Method*, Norwood, MA, Artech House 1995.

[7]   J.W. Goodman, *Introduction to Fourier Optics*, New York, NY, McGraw Hill 1996.

Figure 5: Measurement setup showing WR-10 waveguide, HP8510 MM-Wave system and a Si wafer with 20 period, Au undulator circuits with wavelengths from 20-100µm.